Food Hydrocolloids 165 (2025) 111231

Contents lists available at ScienceDirect

Food Hydrocolloids

journal homepage: www.elsevier.com/locate/foodhyd

Gum Arabic – Same but different: Comparative analysis of structural characteristics and emulsifying properties of 20 *Acacia senegal* samples of various qualities

Frederike Kersten [a], Désirée Martin [b], Ulrike S. van der Schaaf [b,**], Daniel Wefers [a,*]

[a] Institute of Chemistry, Food Chemistry, Martin Luther University Halle-Wittenberg, Kurt-Mothes-Str. 2, 06120, Halle (Saale), Germany
[b] Karlsruhe Institute of Technology, Institute of Process Engineering in Life Sciences – Food Process Engineering, Gotthard-Franz-Str. 3, Building 50.31, 76131, Karlsruhe, Germany

ARTICLE INFO

Keywords:
Acacia senegal
Monosaccharide composition
Molecular structure
Emulsion stability
Molecular weight
Correlation

ABSTRACT

Gum Arabic, an exudate from *Acacia senegal*, is very commonly used for the stabilization of aroma oil and beverage emulsions due to its high emulsifying capacity. However, differences in gum Arabic quality and its relation to the molecular structure are not yet fully understood. In this study, we analyzed the structural characteristics and functional properties of 20 gum Arabic samples of various qualities to investigate the relation between molecular structure and functionality.

First, an improved hydrolysis protocol for a valid determination of the monosaccharide composition of gum Arabic by HPAEC-PAD was established. The application of this method showed that previous monosaccharide compositions potentially underestimated neutral sugars and overestimated uronic acids. The gum samples were subsequently analyzed for their monosaccharide composition, protein content, molecular weight, and molecular weight distribution as well as the radius of gyration and hydrodynamic radius. O/W emulsions with weighted orange oil were prepared from all samples and their initial droplet size distribution and viscosity were determined. By using Pearson correlation tests, we were able to demonstrate that rhamnose content and the rhamnose/galactose ratio positively correlate with the molecular mass M_W. The molecular weight M_W itself correlated with the viscosity of the emulsion, while the protein content anticorrelated with the droplet size distribution $x_{90,3}$. Altogether, we provide a comprehensive and detailed data set on various gum Arabic samples which establishes correlations between individual structural parameters and emulsion properties. However, explaining quality and long-term stability requires a deeper understanding of the molecular structure, emulsion formation, and stabilization processes.

1. Introduction

Gum Arabic (GA) is a gum exudate obtained mainly from *Acacia senegal* growing within the gum belt south of the Sahara, Africa. After picking, the gum is either cleaned and kibbled or dissolved, centrifuged and spray-dried or roller-dried to increase the solubility, remove impurities, and improve handling (Williams & Phillips, 2021). GA can be used for a wide range of applications, from food additive to adhesive to binding agent. Due to its amphiphilic character, it is commonly used as an emulsifier and stabilizer for essential oils and flavors in beverages (Dickinson et al., 1988; Mirhosseini et al., 2008; Ray et al., 1995). Despite wide use of GA and overall excellent technofunctional properties, it remains relatively unclear why functional differences can be observed between different GA batches. A profound understanding of the structure is necessary to grasp this dependency.

GA from *A. senegal* consists of more than 90 % hyperbranched polysaccharides, which are bound to a small protein portion of approx. 2 % (Gashua et al., 2015; Randall et al., 1988; Renard et al., 2006). The polysaccharide domain is usually present as calcium, magnesium and/or potassium salt. It is composed of (1 → 3)-linked β-D-galactopyranose residues which are highly branched at (mainly) position *O*6, but also at position *O*2 and/or *O*4. The side chains are very heterogeneous and contain β-D-galactopyranose, α-L-arabinofuranose, α-L-rhamnopyranose, β-D-glucuronic acid and/or 4-*O*-methyl-D-glucuronic acid units in varying portions and linkages (Nie et al., 2013; Street & Anderson, 1983).

* Corresponding author.
** Corresponding author.
E-mail addresses: ulrike.schaaf@kit.edu (U.S. van der Schaaf), daniel.wefers@chemie.uni-halle.de (D. Wefers).

https://doi.org/10.1016/j.foodhyd.2025.111231
Received 22 November 2024; Received in revised form 31 January 2025; Accepted 15 February 2025
Available online 18 February 2025

Abbreviations

AG	Arabinogalactan
AGP	Arabinogalactan protein
ANOVA	Multifactorial analysis of variance
Ara	Arabinose
DSD	Droplet size distribution
GA	Gum Arabic
Gal	Galactose
GlcA	Glucuronic acid
GP	Glycoprotein
HPAEC-PAD	High performance anion exchange chromatography with pulsed amperometric detection
HPSEC-RI/UV/MALLS	High performance size exclusion chromatography with refractive index, UV/Vis and multi-angle laser light scattering detection
MeGlcA	4-*O*-Methyl-glucuronic acid
Rha	Rhamnose
TFA	Trifluoroacetic acid

The carbohydrate units are linked to the protein domain via *O*-glycosidic bonds to hydroxyproline or serine, which are the main amino acids in the protein domain of GA. Additionally, Akiyama et al. (1984) and Qi et al. (1991) showed that oligoarabinosides are also bound to the protein via *O*-glycosidic linkages. Based on the described composition, the spatial structure of GA was described as wattle blossom type (Connolly et al., 1988; Mahendran et al., 2008). More recent studies analyzed the architecture of GA using size exclusion chromatography with multiangle laser light scattering, small angle neutron scattering (SANS) and small angle x-ray scattering (SAXS), and described the spatial structure more detailed as a thin, disc-like shape being highly flexible (Isobe et al., 2020; Renard et al., 2012; Sanchez et al., 2008).

GA contains several glycoprotein fractions which differ significantly in their charge, their molecular mass, or their hydrophobicity. Using hydrophobic interaction chromatography, arabinogalactan (AG, ~90 wt % with 1 % protein), arabinogalactan protein (AGP, ~10 wt% with 10 % protein) and glycoprotein (GP, ~1 wt% with 25–65 % protein) can be separated (Osman et al., 1994; Randall et al., 1989; Renard et al., 2006). The variety of structural characteristics of these components results in differences in amphiphilic character and emulsifying properties of these fractions. For example, the protein-rich fractions with a higher molecular weight are described as particularly responsible for stabilization of a disperse phase (Atgié et al., 2019; Randall et al., 1988). It is assumed that the hydrophobic protein domains bind irreversible to the oil droplet surface and the hydrophilic polysaccharide chains extend into the aqueous solution, stabilizing the droplets via extension of the distance between them and electrostatic repellence of negatively charged carboxylates (Atgié et al., 2019; Padala et al., 2009).

It is not yet fully understood why some batches of GA show poor long-term emulsion stability. Xiang et al. (2015) and Isobe et al. (2020) suggested that the aggregation of GA on the droplet surfaces is the main cause of coalescence but did not link this observation to specific structural features. Karamalla et al. (1998) attempted to establish quality parameters analyzing a variety of *Acacia senegal* gums by investigating characteristics such as moisture, ash, nitrogen and uronic acid content, specific rotation, pH, viscosity, and viscosity average molecular weight. However, none of these parameters could be considered an adequate quality criterion. Furthermore, parameters such as the monosaccharide composition, molecular weight, or droplet size distributions of emulsions stabilized with the samples were not analyzed. In subsequent publications, it was suggested that the content and molecular mass of the proteinaceous components in *A. senegal* gums could be linked to better emulsifying properties and interfacial behavior (Al-Assaf et al., 2009; Castellani et al., 2010). However, the polysaccharide composition was not analyzed and only a small number of samples were examined in these studies, which prevents a statistically reliable statement. The same applies to the results of Al-Assaf et al. (2003), who investigated the relationship between the long-term stability of GA emulsions and the molecular weight or molecular size distribution of the commercial gums used as emulsifier. They implemented an acceleration test to design a categorization of gum samples in different emulsifier qualities based on the droplet size distribution change. They stated that the functionality and thus the quality of GA appears to depend both on the protein content and on the spatial and molecular profile of the polysaccharide domains (Al-Assaf et al., 2003). However, as mentioned above, the polysaccharide composition was scarcely analyzed for multiple samples. Furthermore, the methods to analyze the contents of the different monosaccharides varied and were not adjusted for GA. Consequently, the correlation between the monosaccharide composition and other parameters (as well as the quality) is unknown.

Therefore, we tested different conditions for monosaccharide composition analysis and subsequently systematically analyzed the structural composition, the molecular mass, and the functional properties of 20 commercial GA samples. Samples with five distinct quality levels, which the suppliers quantified according to the procedure described by Al-Assaf et al. (2003), were used. In this analysis, the quality of a GA sample is accessed by using a heat stress test, wherein a previously prepared emulsion is stored at 60 °C for seven days. The droplet size distribution is then measured as an indicator of quality (Al-Assaf et al., 2003). It can be assumed that the quality of the GA correlates with its chemical properties and long-term emulsion stability. So, we correlated the individual structural and technofunctional parameters with each other to identify relationships between molecular characteristics of GA and its emulsifying properties.

2. Materials and methods

2.1. Materials

Spray dried (commercial) GA samples as well as kibbled GA were provided by Willy Benecke GmbH (Hamburg, Germany) and ADM Wild Europe GmbH & Co. KG (Eppelheim, Germany). The specification and classification of the samples into quality levels 1-very good emulsion stability to 5-average emulsion stability was made by the suppliers. Samples 1–7 and 14–18 were spray-dried samples, whereas samples 8–13 and 19, 20 were unprocessed samples. Prior to analysis, the unprocessed, kibbled gum samples were milled and adhering impurities (bark, fibres, small stones) were removed from the unprocessed samples. Gum solutions were prepared in ultrapure water, heated for a maximum of 1 h at 60 °C and centrifuged at 4250 rpm for 10 min at 25 °C. The supernatant was used for further analyses.

2.2. Structural characterization

Moisture content and dry mass was determined via differential weighing after drying at 105 °C for 4 h (spray-dried GA) and for 5 h (kibbled GA). The dried samples were further used to quantify the ash content according to FAO (1990, pp. 23–25).

2.2.1. Acidic hydrolysis for monosaccharide composition analysis

To investigate the impact of hydrolysis time and acid type on the yield of neutral sugars and uronic acids, three different treatments were used for acid hydrolysis of GA.

Sulphuric acid (H_2SO_4) hydrolysis was based on the procedure described by (Saeman et al., 1945). Briefly, 2.5 mg GA were hydrolyzed with H_2SO_4 (500 μL, 1,6 M) at 100 °C for 3 h. The solutions were filtered (PTFE, 0.45 μm) and an aliquot was neutralized with 4 M sodium hydroxide (NaOH). After dilution, the sample was analyzed by high performance anion exchange chromatography with pulsed amperometric

detection (HPAEC-PAD) as described below.

Trifluoroacetic acid (TFA) hydrolysis was executed according to De Ruiter et al. (1992) with minor modifications. Briefly 0.1 g GA was hydrolyzed with TFA (500 µl, 2 M) at 121 °C for different times varying from 0 to 90 min in 5 min steps. After evaporation of the acid and co-evaporation with ethanol, the monosaccharides were dissolved in ultrapure water, diluted, and used for HPAEC-PAD analysis (see below).

Methanolysis was performed as described by De Ruiter et al. (1992), modified by Wefers and Bunzel (2015). In brief, 0.1 g of GA were hydrolyzed with hydrogen chloride in methanol (500 µl, 1.25 M) at 80 °C for 16 h. After evaporating the liquid, the residue was treated with 2 M TFA as mentioned above.

2.2.2. Neutral sugar and uronic acid composition

The monosaccharide and uronic acid compositions of the GA hydrolysates were analyzed by HPAEC-PAD on a Dionex ICS-3000 system (ThermoFisher Scientific, Germany) equipped with a CarboPac PA-20 column (150 × 3 mm, 6.5 µm particle size, ThermoFisher Scientific, Germany) at 30 °C. Separation of 10 µL of diluted samples was carried out at a flow rate of 0.4 mL/min with ultrapure water (A), 0.2 M NaOH (B) and 0.2 M NaOH plus 0.2 M sodium acetate (C) using the following gradient conditions: 0–12 min isocratic 15 % B, 12–15 min linear to 100 % B, 15–25 min linear to 100 % C, 25–30 min isocratic 100 % C and 30–40 min isocratic 100 % B. Before every run, the column was equilibrated with 15 % B for 15 min.

Qualification was carried out by comparing the retention time of reference substances and quantification was done via external calibration.

2.2.3. Protein content

Protein content of GA was calculated based on the quantification of NH_4^+ after Kjeldahl digestion as described by Urbat et al. (2019). NH_4^+ content was analyzed with an ammonia selective gas membrane electrode (Metrohm, Germany). Using the molar masses the percentage of NH_4^+ was converted into percentage of nitrogen %N. %N multiplied with a protein conversion factor of 6.60 determined by Anderson (1986) results in the percentage of protein content.

2.3. Molecular size distribution

High performance size exclusion chromatography with refractive index detection (1260 Infinity II, Agilent Technologies, Santa Clara, CA), UV/Vis detection at 214 nm (1100 Series, Agilent Technologies, Santa Clara, CA), and multi-angle laser light scattering detection (SLD7100, PSS polymer solutions, Germany) (HPSEC-RI/UV/MALLS) was used to analyze the molecular mass and size distribution of the GA samples. The MALLS instrument was calibrated using standard pullulan PUL110K (Agilent Technologies, Santa Clara, CA) and the RI detector was used as a concentration-dependent detector to calculate the molecular mass. An Agilent HPLC system (1100 Series, Agilent Technologies, Santa Clara, CA) equipped with a TSKgel G5000 PWXL column (30 cm × 7.8 mm i.d., 10 µM particle size, 100 nm pore size, Tosoh Bioscience GmbH, Germany) was used for separation. A 0.2 M NaCl solution was used as eluent at a flow rate of 0.4 mL/min. The separation was carried out at 40 °C and the RI detector was operated at 35 °C. The samples were dissolved in eluent (final concentration: 1.0 g/L).

M_W (weight average molecular mass) and R_G (radius of gyration) were calculated using WinGPC software (PSS SLD7100, PSS polymer solutions, Germany). The dn/dc was calculated for each sample using a single-point calibration, because this allows a more individualized and accurate analysis of the samples. The obtained values for samples 1–18 ranged from 0.138 to 0.149 mL/g (average: 0.142 ± 0.007 mL/g). Sample 19 and 20 were outliers (as in all analyses) with values of 0.124 and 0.126. To verify the robustness of the single-point calibrations, it was compared to a 5-point calibration and the refractive index increments showed a very small deviation of 0.7 %.

2.4. Measurement of hydrodynamic radius

The hydrodynamic radius of GA was determined using a particle analyzer (SZ-100, HORIBA GmbH, Kyoto, Japan) and disposable cuvettes (polystyrene, 10 x 10 × 45 mm). For this purpose, GA solutions were diluted to a concentration of 1 wt%. For each sample, 20 measurements were carried out for 60 s at a temperature of 25 °C. The distribution of the particles was set to "monodisperse" with a broad size distribution.

2.5. Preparation of gum Arabic-stabilized emulsions

Aroma oil-in-water emulsions were prepared by dispersing 10 wt% weighted orange oil (disperse phase) in a 10 wt% GA solution (continuous phase). The orange oils Essential and Brazilian were mixed in a ratio of 1:5 as the disperse phase. To adjust the density of orange oil and water, glycerol ester was dissolved in the orange oil mixture at a ratio of 1:1. In this study, only the weighted orange oil was used, which is referred to as orange oil in the following. The orange oil (20 g) was dispersed in the continuous phase (180 g) in a 400 mL beaker using an Ultraturrax T-25 digital high-speed mixer (IKA® Werke GmbH und Co. KG, Staufen, Germany) at a speed of 10.000 rpm for 30 s. The emulsion premixes were then further dispersed for 2 min at the same speed. Fine emulsions were obtained by homogenizing the coarse emulsions with a high-pressure homogenizer (Microfuidizer M-110 EH, Microfluidics, Newton, MA, USA) at 800 bar for two passages. Each emulsion was prepared in triplicate.

2.6. Measurement of droplet size distribution

The droplet size distribution (DSD) of the prepared aroma oil emulsions was determined by static laser light scattering using a HORIBA LA-950 Particle Analyser (Retsch Technology, Haan, Germany). The results are presented as the cumulative volume distribution Q_3. In all emulsions, the refractive indices were set to n = 1.470 for orange essential oil and to n = 1.333 for water. Droplet size determination followed the Mie theory. All measurements were conducted in triplicate at room temperature. One parameter that can be used from the drop size distribution is $x_{90,3}$. The $x_{90,3}$ is a characteristic value indicates that 90 % of the droplets are smaller than or equal to this value in relation to the droplet volume. It is one typical parameter used to compare the emulsion stabilizing properties of emulsifiers.

2.7. Measurement of viscosity

The dynamic viscosity η of the GA solutions were measured with a Modular Compact Rheometer (Physica MCR 301, Anton Paar GmbH, Graz, Austria) with the double-gap geometry DG26.7. To create constant measuring conditions, each sample was given 5 min to equilibrate at a temperature of 25 °C before the measurement. The shear rate $\dot{\gamma}$ was increased logarithmically from 1 s^{-1} to 1000 s^{-1} in 19 measuring points. The dynamic viscosity was read off at a shear rate of 1000 s^{-1}.

2.8. Statistical analyses

Every sample preparation was made in triplicate. If not specified otherwise, all analyses were conducted at least three times per independent test. All data was assessed via multifactorial analysis of variance (ANOVA) and a Scheffe test as a post hoc test. Dissimilarities in the samples were considered statistically relevant at a level of $p \leq 0.05$. The software OriginPro 2020 (OriginLab Corp., Northampton, MA, USA) was used for the statistical analyses, calculation of averages, standard deviations, and Pearson correlation tests. To correlate the structural properties with one another, the results of the respective dry weight contents were used. To correlate the structural properties with the technofunctional properties, the individual contents in whole gum were

used.

3. Results and discussion

3.1. Structural characterization

For a quantitative analysis of all monosaccharides, the selection of a suitable acid hydrolysis procedure is crucial. Various protocols for releasing the monosaccharides from GA and different analytical methods have been used before. Previous studies mainly applied different modifications of a sulphuric acid hydrolysis combined with HPLC-RI or HPAEC-PAD analysis of neutral sugars and photometric determination of uronic acids (Aoki et al., 2007; Randall et al., 1989). More recent publications primarily used hydrolysis with TFA or a combination of methanolysis and TFA hydrolysis (subsequently referred to as methanolysis) and analyzed the liberated monosaccharides with GC-FID/MS or HPAEC-PAD. Again, photometry was used for the analysis of the uronic acid content in some cases (Gashua et al., 2015; Lopez--Torrez et al., 2015; Qi et al., 1991). Altogether, various approaches have been used, but a systematic investigation to obtain the optimal conditions for the monosaccharide composition analysis of GA has not been conducted. Therefore, we investigated the impact of hydrolysis time and acid type on the yield of neutral sugars and uronic acids in GA. HPAEC-PAD was used because it allows for a sensitive detection and quantification of all neutral sugars and uronic acids.

Fig. 1 shows the chromatograms of GA sample 9 after hydrolysis with TFA hydrolysis, methanolysis, and H_2SO_4 hydrolysis. As expected, the sample contained rhamnose, arabinose, galactose, 4-*O*-methyl-glucuronic acid, and glucuronic acid. However, after H_2SO_4 and TFA hydrolysis, a large peak was detected at 26.3 min which could not be assigned to any monosaccharide or uronic acid. By using HPAEC-PAD/MS^2, the compound was identified as an incompletely cleaved disaccharide containing galactose and glucuronic acid ($[M+Li]^+ = m/z$ 363). Therefore, H_2SO_4 and TFA hydrolysis were not able to fully cleave bonds containing glucuronic acid. The chromatogram obtained after methanolysis demonstrated that this method cleaved the disaccharide efficiently. Furthermore, the peak intensities of galactose and glucuronic acid increased significantly after methanolysis in comparison to the results after TFA hydrolysis (60 min) and H_2SO_4 hydrolysis.

These results are in good agreement with those of De Ruiter et al. (1992) who emphasized the superiority of methanolysis over classical acid hydrolysis with sulphuric acid or TFA for hydrolyzing polysaccharides containing uronic acids. However, methanolysis contains an additional step which includes heating in acidic conditions. Thus, it may lead to an increased degradation of liberated monosaccharides. Therefore, we analyzed the monosaccharide contents after methanolysis and TFA hydrolysis to identify optimized conditions for the analysis of GA. H_2SO_4 hydrolysis was not further investigated, because it leads to an increased destruction of monosaccharides compared to TFA hydrolysis. The contents of rhamnose, arabinose, galactose, 4-*O*-methyl-glucuronic acid, and glucuronic acid after different times of methanolysis and TFA hydrolysis are shown in Fig. 2. The results clearly demonstrate that a short TFA hydrolysis achieved the highest yields for arabinose and rhamnose. After longer hydrolysis times these monosaccharides were slightly degraded. Significantly less arabinose and rhamnose was quantified after methanolysis. These results suggest that the two monosaccharides as well as their methyl glycosides are less stable under acidic conditions. In addition, the results show that arabinose and rhamnose are rapidly released which may also contribute to their quick degradation under acidic conditions. The rapid release could be caused by the positioning of these monosaccharides in GA, as it can be assumed that they particularly occur in side chains and at terminal positions of the carbohydrate moieties (Akiyama et al., 1984; Mahendran et al., 2008; Nie et al., 2013). For the determination of galactose, methanolysis and TFA hydrolysis are somewhat similarly suited, because the contents after 30 min of hydrolysis were almost identical. Longer hydrolysis times are most likely beneficial, because galactose is present as β-pyranose and predominantly located in the polysaccharide backbone which could cause a higher resistance to acid hydrolysis and degradation. As mentioned above, glucuronic acid was detected much more efficiently with methanolysis. As described by De Ruiter et al. (1992), this procedure enables a better cleavage of the glycosidic bonds containing glucuronic acid and at the same time improved stabilization of the free acids as methyl glycosides. Based on the results, all 20 GA samples were analyzed by using a short 20 min TFA hydrolysis for rhamnose and arabinose and methanolysis followed by 60 min TFA hydrolysis for galactose, glucuronic acid, and 4-*O*-methyl-glucuronic acid. Methanolysis was selected because the above-mentioned dimer of galactose and glucuronic acid was clearly present in all TFA hydrolysates.

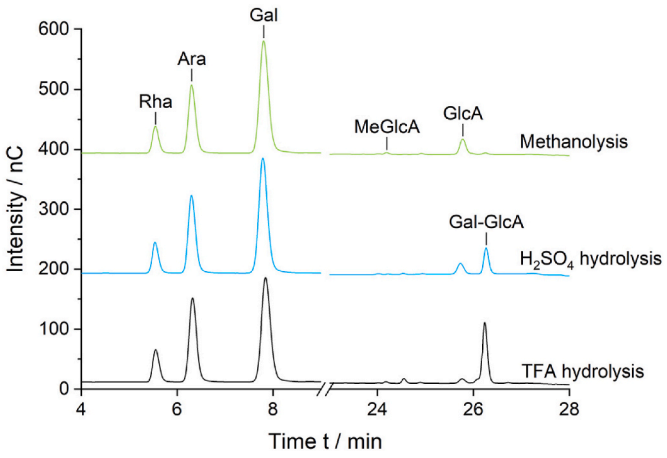

Fig. 1. HPAEC-PAD chromatograms of GA sample 9 after different hydrolysis methods, Rha – rhamnose, Ara – arabinose, Gal – galactose, MeGlcA – 4-O-methyl-glucuronic acid, GlcA – glucuronic acid, Gal-GlcA – dimer composed of galactose and glucuronic acid.

The analytical data collected on the monosaccharide and uronic acid composition as well as protein, moisture, ash content, and macromolecular characteristics (molar mass, radius of gyration, hydrodynamic radius) of each sample are given in the supporting information (Table S5). Only slight differences in the sugar composition of the samples were observed. On average, GA samples contained 10.5 ± 0.2 % rhamnose, 27.3 ± 0.6 % arabinose, 42.4 ± 0.8 % galactose, 0.7 ± 0.1 % 4-*O*-methylglucuronic acid and 9.3 ± 0.2 % glucuronic acid in the dry mass (90.3 ± 1.9 % total carbohydrates in dry mass). Notably, sample 19 and sample 20 deviate significantly from the average as they show higher levels of rhamnose and glucuronic acid and lower levels of arabinose and 4-*O*-methylglucuronic acid. The other samples do not show significant differences between each other.

The monosaccharide yields and monosaccharide portions were comparable to literature data, however, our analyses led to slightly higher contents of neutral sugars, especially for galactose. For example Randall et al. (1989) and Lopez-Torrez et al. (2015) quantified about 36 % galactose (based on dry weight). Furthermore, the uronic acid contents in the literature were significantly higher, between 19.5 and 23.7 % (based on dry weight) compared to 10 %, the content we were able to detect by using HPAEC-PAD (Gashua et al., 2015; Randall et al., 1988, 1989). One could argue that some uronic acids are not detected after acid hydrolysis due to degradation in the acidic environment. This is most likely the case as water, ash, protein, and the sum of monosaccharides do not always add up to 100 %. However, the differences which can be attributed to this factor are clearly lower than 10 %, so it can be assumed that uronic acid contents in the literature are overestimated. This could be caused by the lower selectivity of the photometric analysis of uronic acids, because other sugars can also react with the reagent and interfere with the quantification (Filisetti-Cozzi & Carpita, 1991). The higher contents of galactose in our study compared to

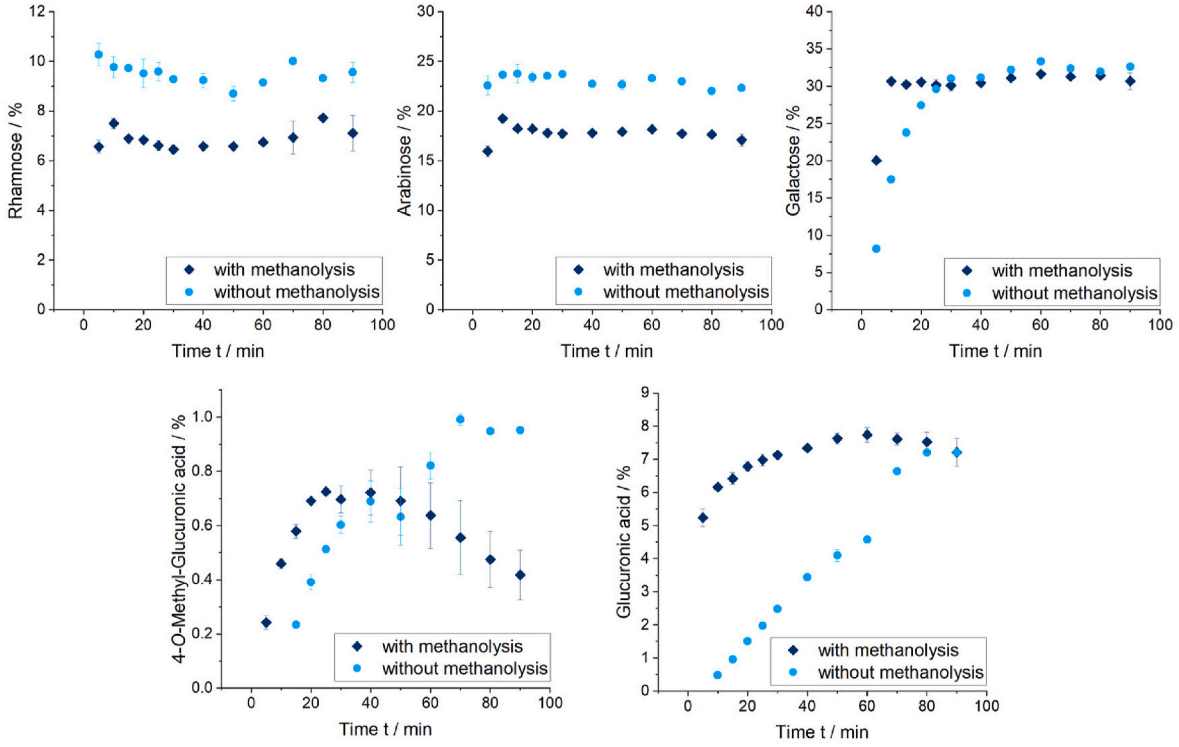

Fig. 2. Contents of rhamnose, arabinose, galactose, 4-*O*-methyl-glucuronic acid, and glucuronic acid after different times of TFA hydrolysis with and without preceding methanolysis (16 h, 80 °C). Monosaccharide contents were determined by HPAEC-PAD and all analyses were carried out in duplicate.

others can also be explained by the application of H_2SO_4 hydrolysis in the literature: As shown in Fig. 1, a disaccharide of galactose and glucuronic acid remains when H_2SO_4 (or solely TFA) is used for hydrolysis of GA. This leads to lower galactose contents, while the contents of arabinose and rhamnose may also be impaired due to degradation. Therefore, our results suggest that neutral sugar contents and uronic acid contents in GA were slightly underestimated or overestimated in the literature, respectively.

The GA samples were also analyzed for free monosaccharides. Small amounts of rhamnose, arabinose and galactose were detected in all samples, and total free monosaccharides ranged from 0.07 to 0.60 % in dry mass. The presence of these components may be derived from enzymatic activity in the native gum or thermal influence during storage and processing.

The protein and mineral contents of the GA samples were in good agreement with literature data (Randall et al., 1988, 1989). On average,

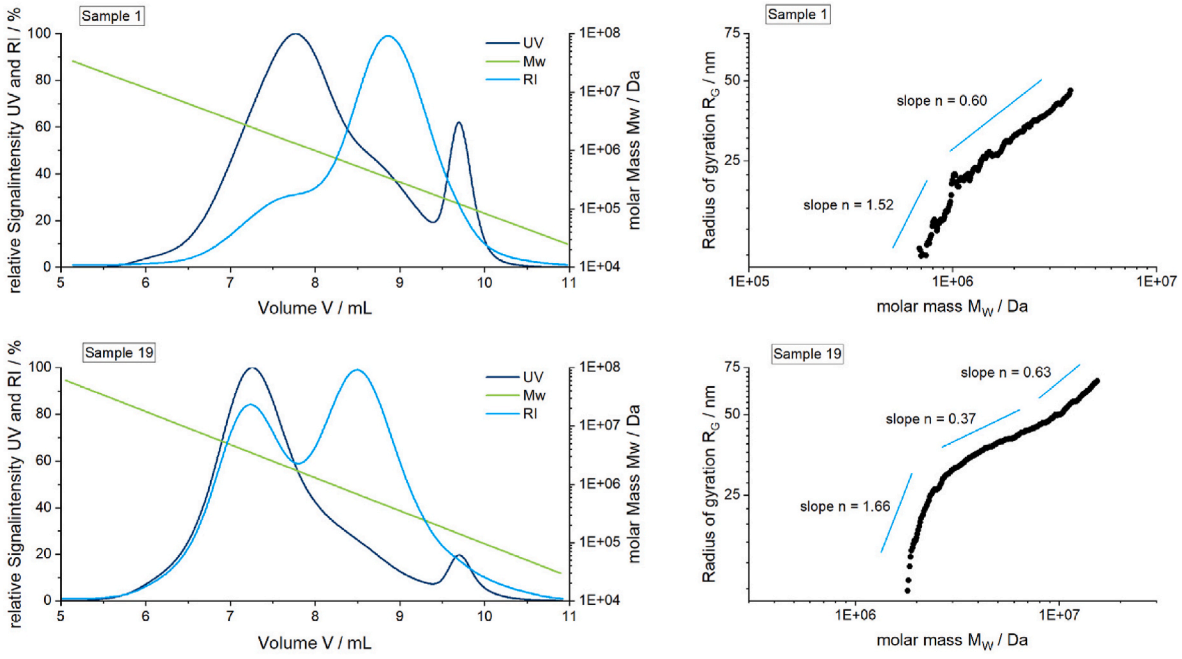

Fig. 3. *HPSEC-RI/UV/MALLS elution profiles of two selected GA samples and their resulting radius of gyration R_G as function of the molar mass M_W, where the indicated numbers correspond to the power n, e.g. slopes of each line ($R_G \propto M_W^n$).*

the samples contained 2.5 ± 0.1 % protein in dry matter and 4.0 ± 0.0 % minerals in dry matter. The samples differ slightly in their protein content, ranging from 2.1 to 3.0 %. Samples 19 and 20 again show exceptional mineral contents above the average which is in good agreement with their higher contents of glucuronic acid.

The GA samples differed most clearly in their molecular weight distribution and radius of gyration R_G as well as their HPSEC elution profile. The elution profiles of two selected GA samples are shown in Fig. 3 (all elugrams are shown in Figs. S1–S20). All GA samples show three overlapping molecular fractions corresponding well with previous findings (Al-Assaf et al., 2003; Connolly et al., 1988; Gashua et al., 2015; Picton et al., 2000; Randall et al., 1989). For most samples, the first fraction (eluting from about 5 mL to 8 mL) takes up only a small portion of the total GA, indicated by the low intensity in the RI detector. However, this fraction showed an intense peak in the UV and the light scattering detector, which suggests a high molecular weight population with a large radius of gyration and an increased protein content. The second fraction (eluting from 8 mL to 9.4 mL) makes up the majority of GA, but shows a less intense UV and light scattering signal compared to fraction 1. Thus, these molecules are smaller and have a lower protein content. The third fraction (eluting from 9.4 mL to 10.5 mL) shows little to no signal in the RI detector and the light scattering detector, but intense UV absorption at 214 nm. Those molecules are small and high in protein, but only account for a minority of the total gum. These results are in good agreement with the different glycoproteins described for GA: AGP, AG and GP (Al-Assaf et al., 2003; Connolly et al., 1988; Randall et al., 1989). Although the whole gum samples showed overall comparable elution profiles, they differed in their molecular characteristics (M_W, M_n, R_G, and polydispersity D): The weight-average molecular weight M_W of the whole peak ranged from 422 kDa to 2300 kDa, while R_G ranged from <10 nm to 36 nm (Table S1). Fraction 1 (Table S2) and fraction 2 + 3 (Table S3) also showed strong variations in their portions and characteristics. Especially sample 19 and 20 showed a clearly different molecular distribution. The most pronounced difference is that glycoproteins in fraction 1 are considerably larger and represent a higher proportion of the total gum than molecules of fraction 1 in the other samples. In previous publications, this fraction is described responsible for the functionality of GA (Al-Assaf et al., 2003; Castellani et al., 2010).

Due to the power law describing the M_W dependence of R_G ($R_G \propto M_W^n$), information on the conformation can be derived from the value n, as the coefficient depends on the polymer shape, solvent-polymer-interactions, and temperature. Values of n = 0.33 are described as spherical, n = 0.5–0.6 for a flexible, random coil and n = 1 for rod-like chains (Burchard, 1999; Picton et al., 2000). Fig. 3 shows the log-log plot R_G vs. M_W and the corresponding slopes for two different samples (mass ranges and slopes for all samples are shown in Table S4). Plotting is only possible for the high molecular mass polymers of fraction 1 due to the sensitivity of MALLS detection and low polydispersity of the AGP fraction. Samples 1 to 18 showed similar plots, exhibiting mostly two slopes with mean values of 0.97 for a molar mass range of $4 \times 10^5 - 2 \times 10^6$ Da and 0.65 for $2 \times 10^6 - 5 \times 10^6$ Da for the 18 samples. Thus, the smaller polymers in the AGP fraction appear to form rod-like chains and bigger molecules of this fraction are present as flexible, random linear-coils. These findings agree with previously published data (Isobe et al., 2020; Renard et al., 2012). Samples 19 and 20 showed generally higher M_W polymers in AGP fraction and their log-log plots exhibited three slopes, indicating rod-like and random coil shapes but contrary to the other samples also showing spherical polymers.

To further characterize the samples, the hydrodynamic radius R_H was measured. In contrast to the radius of gyration R_G, which is determined by chromatography and static light scattering, the hydrodynamic radius was determined by dynamic light scattering. R_G describes the mean distance of the scattering sites to the center of gravity of a molecule. R_H reflects the size of a molecule diffusing in solution and is greatly influenced by the solvent molecules. R_G and R_H both characterize the size but are not synonymous. In comparison to the value of R_H, the way in which R_G is calculated makes its value slightly more reliant on the structure of the molecule of interest.

For the GA samples R_H values displayed a wide range from 63 nm up to 420 nm. Especially the unprocessed samples showed lower values (mean value 143 nm) in comparison to the spray dried samples (mean value 295 nm). As described previously, high R_H values can be associated with the aggregation of the different molecular species of GA during spray drying (Li et al., 2009). Sample 19 and 20 showed again exceptional values as their hydrodynamic radii are high for unprocessed GA. Overall the measured hydrodynamic radii are in agreement with literature data (Isobe et al., 2020; Li et al., 2009; Vinayahan et al., 2010). The quotient of R_G/R_H is used to describe the shape of GA molecules (Van de Sande & Persoons, 1985). For all samples, the quotient yielded very low values ranging from 0.024 to 0.244 (Table S4), due to R_H being considerably greater than R_G. The difference in the radii can be explained by the different solutions used during measurements. In the aqueous solution used for the R_H analysis, the polymers are more extended, branches reach further into the solution and cause high R_H values. The saline solution used as HPSEC eluent provides a more compact structure of GA, as seen in the R_G values.

3.2. Viscosity of gum Arabic solutions

One of the key reasons GA is so highly valued is that it does not significantly increase the viscosity of a solution when dissolved in water. The viscosity enhancing properties of hydrocolloids are caused by their polymeric molecular structure. As the investigated GA samples showed structural differences, effects on the viscosity of the corresponding solutions were expected. Fig. 4 shows the viscosity at a shear rate of 1000 s^{-1} for a 10 wt% solution of all GA samples used in the study.

The viscosity of 18 of the 20 samples was between 0.006 Pa·s and 0.012 Pa·s which is very low despite the relatively high concentration of dissolved material. Two samples (number 19 and 20) however have a significantly higher viscosity of over 0.02 Pa·s. Overall, the measured viscosities correlate with literature values (Li et al., 2009). The higher viscosity values of samples 19 and 20 can be explained by the higher molecular mass of these GA samples (Poh & Ong, 1984). A comparative analysis of the viscosity curves for the various GA samples reveals a high degree of similarity among them. All samples exhibit a slight shear thinning behavior.

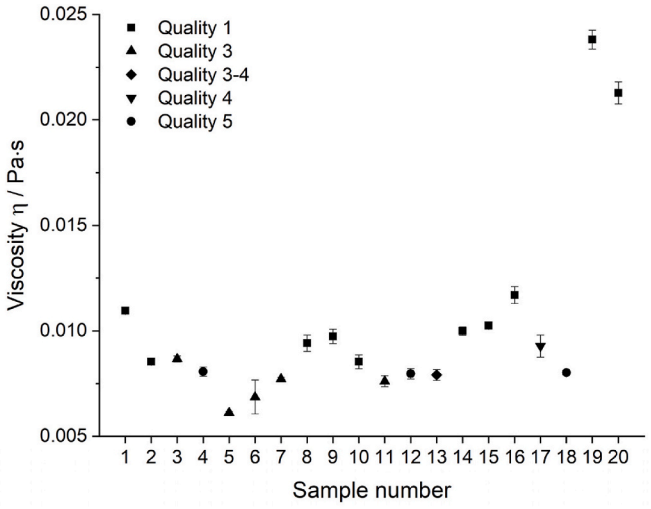

Fig. 4. Viscosity of 10 wt% GA solutions at 1000 s^{-1} shear rate, measured at 25 °C in a double gap.

3.3. Characterization of gum Arabic stabilized aroma oil emulsions

To evaluate the technofunctional properties of the different GA samples, aroma oil emulsions were prepared, and their droplet size distribution was determined. The emulsion formulation and preparation method (high-pressure homogenization) were designed to be close to industrial applications. The characteristic droplet size $x_{90,3}$ of the emulsions is shown in Fig. 5.

The $x_{90,3}$ values were consistently less than 1 μm, making all gums very suitable for stabilizing aroma oils. Such small droplet sizes are often associated with increased stability against creaming and reduced coalescence especially in beverage emulsions (Piorkowski & McClements, 2014). All measured $x_{90,3}$ values were within a narrow range of 0.24–0.49 μm. An analysis of variance (ANOVA) was performed to determine statistically significant differences between the $x_{90,3}$ values. Samples 19 and 20 were significantly different and exhibited notably larger $x_{90,3}$ values in the emulsions. These GA samples were also distinguished by their high molecular mass, large R_G, and high protein content. Moreover, they were also termed as being of excellent quality in the supplier classification. Other than that, samples 4, 5 and 12 showed significant differences, the effect being much smaller, though. The emulsions prepared with these GA samples showed only slightly larger $x_{90,3}$ values than the remaining 15 samples. Interestingly, their quality classification comprises both the labels excellent and only average indicating that maximum droplet size does not correlate with overall performance of GA. Moreover, all these emulsions were stable for several weeks, suggesting that the stability not only depends on the GA used but also on the oil to be emulsified, the overall GA concentration, GA/oil ratio and storage conditions.

3.4. Correlation of structural characteristics with technofunctional properties

In our previous study on sugar beet pectin (SBP), we detected linear correlations between the structural features of the hydrocolloids and their emulsifying properties (Bindereif et al., 2021). For example, there was a strong positive correlation between the characteristic droplet size and a reduced arabinan content. In contrast, the opposite was true for the protein content. The colloidal conformation and the emulsion stabilizing mechanism of GA is described to be somewhat like that of SBP (Bai et al., 2017; Williams et al., 2005). We therefore hypothesized that there would also be linear correlations between the technofunctional properties, i.e. characteristic droplet size and viscosity, and the molecular structural features of GA. To test this assumption, Pearson correlation tests were conducted. This approach allows for the determination of the strength and direction of linear correlations between the various parameters. The Pearson correlation test assumes a normal distribution of the input data. For the presented data, this was only true when samples 19 and 20 were left out. For most parameters, samples 19 and 20 presented outliers to a normally distributed population so that correlation tests were conducted for the remaining 18 samples. In the Pearson correlation tests, the functional parameters "characteristic droplet size" and "viscosity" were tested for a linear relationship with structural parameters. Moreover, various structural parameters were set into correlation with each other. Although free monosaccharides could be a marker for polysaccharide degradation, we found no association between them and any other parameter. Therefore, the contents of free monosaccharides were not considered further. Fig. 6 visualizes the results of individual Pearson tests in a single matrix.

For most of the Pearson tests between either structural parameters or functional and structural parameters, the correlation index (R) is between -0.2 and 0.2. This indicates that there was no linear relationship between the tested parameters. Only few parameters stand out, which are described in more detail in the following.

In terms of structural parameters, strong positive correlations, i.e. positive linear relationships, were found for Rha and Rha/Gal, Ara and Ara/Gal, and GlcA and GlcA/Gal. The quotients of Rha and Gal or Ara and Gal as well as GlcA and Gal reflect the branching of the galactose backbone with the respective monosaccharides or uronic acids. When the portion of one of the monosaccharides increases, so does the corresponding quotient. Moreover, a positive linear correlation was found for the molecular weight M_W with Rha content ($R = 0.69$) and with the quotient Rha/Gal ($R = 0.63$). Both indicate that the large molecular weight of GA samples is mainly caused by a stronger branching of the molecules. This agrees with the results of the monosaccharide characterization after hydrolysis as discussed in chapter 3.1. Regarding the colloidal conformation of the molecules, as mathematically expected, R_G correlates strongly positive with M_W ($R = 0.85$). Thus, molecules with high molecular mass and high Rha content also display a large radius of gyration. Consequently, R_G also correlates positively with Rha ($R = 0.60$) enforcing again that a large extension of the molecules is caused by higher branching.

For R_H, different correlations were found. R_H does not correlate with Rha and Rha/Gal. Instead, a moderate positive correlation with GlcA

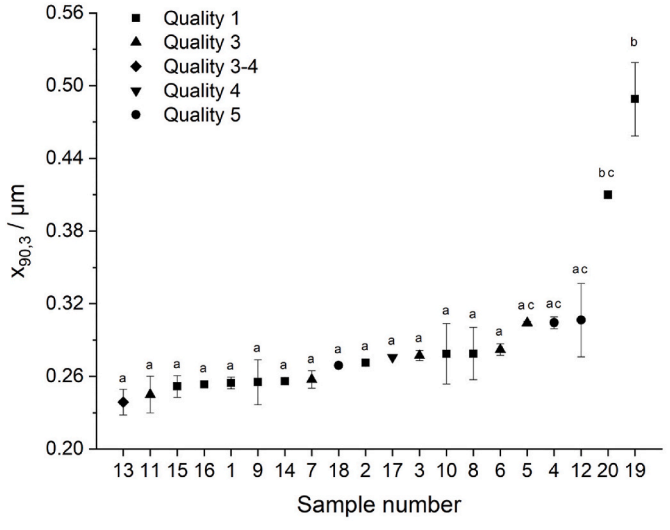

Fig. 5. Characteristic droplet size $x_{90,3}$ in μm of GA stabilized orange oil emulsions. Letters indicate statistically significant differences at a level of $p < 0.05$.

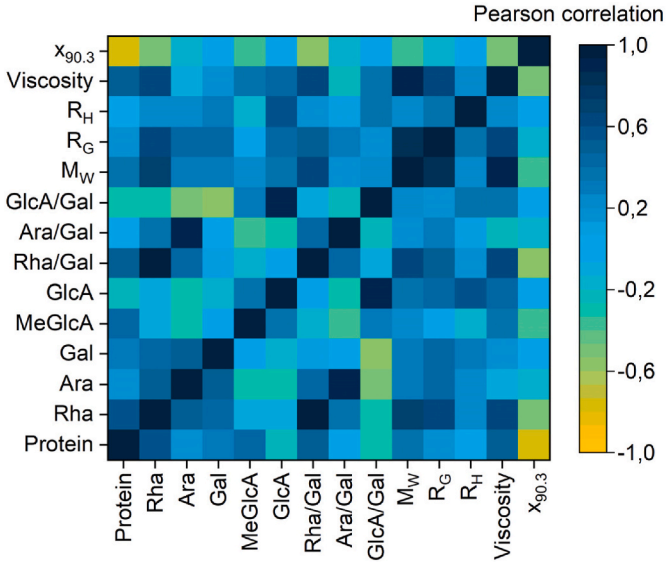

Fig. 6. Matrix of linear Pearson correlations between different structural and functional properties of the GA samples.

was found (R = 0.55), indicating that higher uronic acid content contributes to a larger extension of the molecule. In contrast to R_G, R_H was not determined by chromatography but by dynamic light scattering when the molecule is dissolved in water. Here, the carboxy groups of the uronic acids will be deprotonated promoting intramolecular electrostatic repulsion of the GA molecules and thus an enlarged conformation. During HPSEC, the carboxy groups of the uronic acids were present as sodium adducts so intramolecular electrostatic repulsion can be disregarded. Thus, R_G reflects the actual volume expansion more accurately.

Regarding the technofunctional properties, a strong positive linear correlation between the viscosity of the GA solutions and the average M_W (R = 0.90) as well as a positive linear correlation between viscosity and Rha content (R = 0.61) and Rha/Gal ratio (R = 0.62) of the corresponding GA samples were found. This is in line with established mechanisms that molecules of higher molecular weight increase the viscosity of a solution more strongly. As stated above, the M_W of the GA samples depends on their Rha portion and the branching of the molecules, thus, the solution viscosity also depends on the Rha portion and Rha/Gal, respectively. Yet, the latter two correlations are not as pronounced. To substantiate this finding, Fig. 7 visualizes the dependency of the GA solution viscosity on the samples' molecular mass for all 20 samples, i.e. the 18 samples incorporated in the Pearson test and samples 19 and 20. The linear correlation established by samples 1–18, that is the samples on the left-hand side of the diagram, can clearly be seen. This correlation is further continued by samples 19 and 20 on the right-hand side of the diagram at much higher molecular weights. The reliability of the established linear relationship is highlighted by the high R^2 of 0.81. Moreover, Fig. 7 shows that the samples align according to their emulsion quality, i.e. the long-term emulsion stability as analyzed by the suppliers. But the samples overlap and are not separated satisfactorily as distinguished quality levels. Thus, the molecular mass and, consequentially, the branching of the molecules exceedingly influence the emulsion quality.

Finally, the characteristic droplet size was analyzed for linear correlations with the structural and colloidal parameters as well as the viscosity. As shown in Fig. 6, $x_{90,3}$ is strongly anticorrelated with the protein content (R = -0.78) and moderately with Rha/Gal (R = -0.58) as well as Rha (R = -0.52). A less pronounced negative correlation with the viscosity (R = -0.47) and the Mw (R = -0.36) can also be observed. Most of these parameters are interrelated as the viscosity correlates with M_W and thus Rha and Rha/Gal. Viscosity affects droplet size as high viscosity can both improve droplet break-up, resulting in small droplet sizes, and prevent droplets from coalescing after break-up by reducing droplet movement (Barnea & Mizrahi, 1975; Grace, 1982). Interestingly, the correlation of $x_{90,3}$ with Rha/Gal is stronger than with the viscosity. This suggests that the droplet stabilizing mechanism of strongly branched GA molecules is associated with a better sterical stabilization of oil droplets. For SBP, we were also able to show that a higher portion of neutral pectic side chains resulted in smaller characteristic droplet sizes (Bindereif et al., 2021; Eichhöfer et al., 2023).

The most striking correlation, however, is the one between the characteristic droplet size and the protein content (Fig. 8). Here, a strongly negative relationship exists, showing that higher protein contents result in smaller $x_{90,3}$ values of the emulsions. This aligns with previous studies on GA but contrasts with our results on SBP (Atgié et al., 2019; Bindereif et al., 2021; Randall et al., 1988). One can conclude that despite the previously described similarities between SBP and GA, systematic differences in their droplet stabilizing mechanism must exist (Bai et al., 2017). The complexity of GA's stabilizing mechanism is further highlighted in Fig. 8. The linear correlation observed for samples 1–18 results in a quite high R^2 of 0.88. Samples 19 and 20 are shown alongside the other samples. These two samples stick out in that they display very large droplet sizes despite their comparably high protein content. A reason for this deviation could not be found within the analyzed structural parameters. Consequently, even more investigation on this matter, that is the structure-function relationships of GA, is required.

4. Conclusion

Due to the very complex structure of GA, a detailed and valid structural characterization is a major challenge. We demonstrated that selecting a suitable hydrolysis protocol is crucial for accurately analyzing the monosaccharide composition. Our data suggest that the contents of glucuronic acid and neutral sugars were previously overestimated and underestimated, respectively. The relationship between the structural characteristics and emulsifying properties of GA appears to be an intertwined one. By using our profound data set on the structural and technofunctional features of 20 *Acacia senegal* GA samples, we demonstrated important correlations between individual parameters. Rhamnose and the ratio of rhamnose to galactose were recognized as

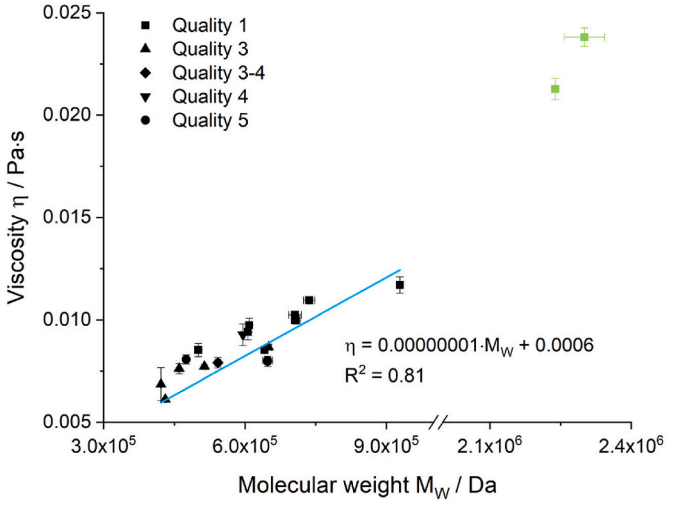

Fig. 7. Correlation between the viscosity of a 10 wt% GA solution at 1000 s^{-1} shear stress, measured at 25 °C in a double gap, and the molecular weight of the corresponding sample; marked in green: sample 19 and 20 (outliers). (For interpretation of the references to colour in this figure legend, the reader is referred to the Web version of this article.)

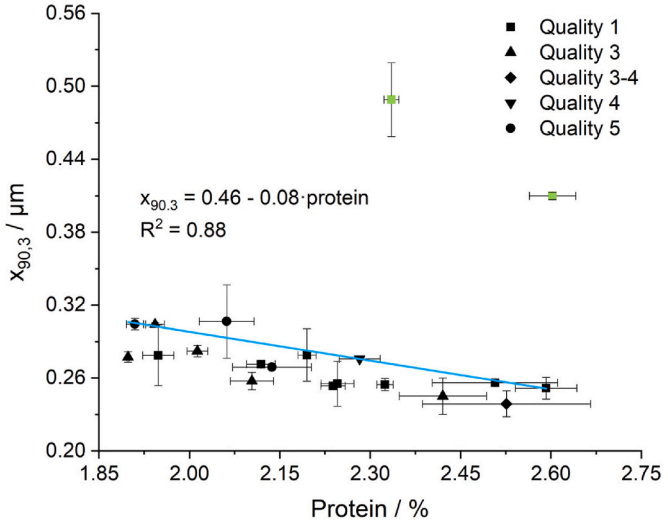

Fig. 8. Measured $x_{90,3}$ values of all aroma oil emulsion samples plotted against the protein concentration of the corresponding GA; marked in green: sample 19 and 20 (outliers). (For interpretation of the references to colour in this figure legend, the reader is referred to the Web version of this article.)

markers for the degree of branching, as both correlated with the molecular mass M_W. The molecular mass and thus the branching of the polysaccharide chains is also interconnected with the radius of gyration R_G and the viscosity: The greater the spatial expansion of the GA molecules, the higher the viscosity of the solution. In addition, the viscosity/M_W ratio was related to the quality levels of the samples, but no distinct separation could be achieved. We also showed that all 20 GA samples were able to achieve droplet size distributions $x_{90,3}$ smaller than 1 μm and are therefore suitable for use in the stabilization of aroma oil emulsions. By comparing the droplet size to the structural features, we could show a strong anticorrelation to the protein content but no connection to quality could be made. These results suggest that emulsion stability using GA depends mostly on the molecular expansion rather than the overall protein content. To obtain more mechanistical information, a more detailed investigation of the molecular structure and interfacial behavior is necessary, which will be in the focus of future studies.

CRediT authorship contribution statement

Frederike Kersten: Writing – original draft, Visualization, Methodology, Investigation, Formal analysis, Conceptualization. **Désirée Martin:** Writing – original draft, Visualization, Methodology, Investigation, Formal analysis, Conceptualization. **Ulrike S. van der Schaaf:** Writing – review & editing, Supervision, Resources, Funding acquisition, Conceptualization. **Daniel Wefers:** Writing – review & editing, Supervision, Resources, Funding acquisition, Conceptualization.

Funding

This research was funded within the framework of IGF project no. 21935 BG of the FEI within the program for promoting the Industrial Collective Research (IGF) of the German Ministry of Economics and Climate Action (BMWK), based on a resolution of the German Parliament.

Declaration of competing interest

The authors declare that they have no known competing financial interests or personal relationships that could have appeared to influence the work reported in this paper.

Acknowledgments

The authors would like to thank Lydia Schütz, Annette Berndt and Markus Fischer for their support in carrying out the numerous experiments.

Appendix A. Supplementary data

Supplementary data to this article can be found online at https://doi.org/10.1016/j.foodhyd.2025.111231.

Data availability

Data will be made available on request.

References

Akiyama, Y., Eda, S., & Katō, K. (1984). Gum Arabic is a kind of arabinogalactan–protein. *Agricultural and Biological Chemistry, 48*(1), 235–237. https://doi.org/10.1080/00021369.1984.10866126

Al-Assaf, S., Katayama, T., & Phillips, G. O. (2003). Quality control of gum Arabic. *Foods and food ingredients journal of Japan, 208*(10), 771–780. Retrieved from https://cir.nii.ac.jp/crid/1522825130237034112.

Al-Assaf, S., Sakata, M., McKenna, C., Aoki, H., & Phillips, G. O. (2009). Molecular associations in acacia gums. *Structural Chemistry, 20*(2), 325–336. https://doi.org/10.1007/s11224-009-9430-3

Anderson, D. M. (1986). Nitrogen conversion factors for the proteinaceous content of gums permitted as food additives. *Food Additives & Contaminants, 3*(3), 231–234. https://doi.org/10.1080/02652038609373585

Aoki, H., Al-Assaf, S., Katayama, T., & Phillips, G. O. (2007). Characterization and properties of *Acacia Senegal* (L.) willd. Var. Senegal with enhanced properties (Acacia (sen) SUPER GUM™): Part 2—mechanism of the maturation process. *Food Hydrocolloids, 21*(3), 329–337. https://doi.org/10.1016/j.foodhyd.2006.04.002

Atgié, M., Masbernat, O., & Roger, K. (2019). Emulsions stabilized by gum Arabic: Composition and packing within interfacial films. *Langmuir: The ACS Journal of Surfaces and Colloids, 35*(4), 962–972. https://doi.org/10.1021/acs.langmuir.8b02715

Bai, L., Huan, S., Li, Z., & McClements, D. J. (2017). Comparison of emulsifying properties of food-grade polysaccharides in oil-in-water emulsions: Gum Arabic, beet pectin, and corn fiber gum. *Food Hydrocolloids, 66*, 144–153. https://doi.org/10.1016/j.foodhyd.2016.12.019

Barnea, E., & Mizrahi, J. (1975). A generalised approach to the fluid dynamics of particulate systems part 2: Sedimentation and fluidisation of clouds of spherical liquid drops. *Canadian Journal of Chemical Engineering, 53*(5), 461–468. https://doi.org/10.1002/cjce.5450530501

Bindereif, B., Eichhöfer, H., Bunzel, M., Karbstein, H. P., Wefers, D., & van der Schaaf, U. S. (2021). Arabinan side-chains strongly affect the emulsifying properties of acid-extracted sugar beet pectins. *Food Hydrocolloids, 121*, Article 106968. https://doi.org/10.1016/j.foodhyd.2021.106968

Burchard, W. (1999). Solution properties of branched macromolecules. In *Branched polymers II* (pp. 113–194). Berlin, Heidelberg: Springer. https://doi.org/10.1007/3-540-49780-3_3.

Castellani, O., Guibert, D., Al-Assaf, S., Axelos, M., Phillips, G. O., & Anton, M. (2010). Hydrocolloids with emulsifying capacity. Part 1 – emulsifying properties and interfacial characteristics of conventional (*Acacia Senegal* (L.) Willd. var. Senegal) and matured (Acacia (sen) SUPER GUM™) *Acacia Senegal. Food Hydrocolloids, 24*(2–3), 193–199. https://doi.org/10.1016/j.foodhyd.2009.09.005

Connolly, S., Fenyo, J.-C., & Vandevelde, M.-C. (1988). Effect of a proteinase on the macromolecular distribution of *Acacia Senegal* gum. *Carbohydrate Polymers, 8*(1), 23–32. https://doi.org/10.1016/0144-8617(88)90033-1

De Ruiter, G. A., Schols, H. A., Voragen, A. G., & Rombouts, F. M. (1992). Carbohydrate analysis of water-soluble uronic acid-containing polysaccharides with high-performance anion-exchange chromatography using methanolysis combined with TFA hydrolysis is superior to four other methods. *Analytical Biochemistry, 207*(1), 176–185. https://doi.org/10.1016/0003-2697(92)90520-H

Dickinson, E., Murray, B. S., Stainsby, G., & Anderson, D. M. (1988). Surface activity and emulsifying behaviour of some Acacia gums. *Food Hydrocolloids, 2*(6), 477–490. https://doi.org/10.1016/S0268-005X(88)80047-X

Eichhöfer, H., Bindereif, B., Karbstein, H. P., Bunzel, M., van der Schaaf, U. S., & Wefers, D. (2023). Influence of arabinan fine structure, galacturonan backbone length, and degree of esterification on the emulsifying properties of acid-extracted sugar beet pectins. *Journal of Agricultural and Food Chemistry, 71*(4), 2105–2112. https://doi.org/10.1021/acs.jafc.2c07460

FAO. (1990). *Food and Nutrition Paper No. 49: Specifications for identity and purity of certain food additives*.

Filisetti-Cozzi, T. M., & Carpita, N. C. (1991). Measurement of uronic acids without interference from neutral sugars. *Analytical Biochemistry, 197*(1), 157–162. https://doi.org/10.1016/0003-2697(91)90372-Z

Gashua, I. B., Williams, P. A., Yadav, M. P., & Baldwin, T. C. (2015). Characterisation and molecular association of Nigerian and Sudanese Acacia gum exudates. *Food Hydrocolloids, 51*, 405–413. https://doi.org/10.1016/j.foodhyd.2015.05.037

Grace, H. P. (1982). Dispersion phenomena in high viscosity immiscible fluid systems and application of static mixers as dispersion devices in such systems. *Chemical Engineering Communications, 14*(3–6), 225–277. https://doi.org/10.1080/00986448208911047

Isobe, N., Sagawa, N., Ono, Y., Fujisawa, S., Kimura, S., Kinoshita, K., & Deguchi, S. (2020). Primary structure of gum Arabic and its dynamics at oil/water interface. *Carbohydrate Polymers, 249*, Article 116843. https://doi.org/10.1016/j.carbpol.2020.116843

Karamalla, K., Siddig, N., & Osman, M. (1998). Analytical data for *Acacia Senegal* var. Senegal gum samples collected between 1993 and 1995 from Sudan. *Food Hydrocolloids, 12*(4), 373–378. https://doi.org/10.1016/S0268-005X(98)00005-8

Li, X., Fang, Y., Al-Assaf, S., Phillips, G. O., Nishinari, K., & Zhang, H. (2009). Rheological study of gum Arabic solutions: Interpretation based on molecular self-association. *Food Hydrocolloids, 23*(8), 2394–2402. https://doi.org/10.1016/j.foodhyd.2009.06.018

Lopez-Torrez, L., Nigen, M., Williams, P., Doco, T., & Sanchez, C. (2015). *Acacia Senegal* vs. *Acacia seyal* gums – Part 1: Composition and structure of hyperbranched plant exudates. *Food Hydrocolloids, 51*, 41–53. https://doi.org/10.1016/j.foodhyd.2015.04.019

Mahendran, T., Williams, P. A., Phillips, G. O., Al-Assaf, S., & Baldwin, T. C. (2008). New insights into the structural characteristics of the arabinogalactan-protein (AGP) fraction of gum Arabic. *Journal of Agricultural and Food Chemistry, 56*(19), 9269–9276. https://doi.org/10.1021/jf800849a

Mirhosseini, H., Tan, C. P., Hamid, N. S., & Yusof, S. (2008). Effect of Arabic gum, xanthan gum and orange oil contents on ζ-potential, conductivity, stability, size index and pH of orange beverage emulsion. *Colloids and Surfaces a: Physicochemical and Engineering Aspects, 315*(1–3), 47–56. https://doi.org/10.1016/j.colsurfa.2007.07.007

Nie, S.-P., Wang, C., Cui, S. W., Wang, Q., Xie, M.-Y., & Phillips, G. O. (2013). A further amendment to the classical core structure of gum Arabic (*Acacia Senegal*). *Food Hydrocolloids, 31*(1), 42–48. https://doi.org/10.1016/j.foodhyd.2012.09.014

Osman, M. E., Menzies, A. R., Williams, P. A., & Phillips, G. O. (1994). Fractionation and characterization of gum Arabic samples from various African countries. *Food Hydrocolloids, 8*(3–4), 233–242. https://doi.org/10.1016/S0268-005X(09)80335-4

Padala, S. R., Williams, P. A., & Phillips, G. O. (2009). Adsorption of gum Arabic, egg white protein, and their mixtures at the oil-water interface in limonene oil-in-water emulsions. *Journal of Agricultural and Food Chemistry, 57*(11), 4964–4973. https://doi.org/10.1021/jf803794n

Picton, L., Bataille, I., & Muller, G. (2000). Analysis of a complex polysaccharide (gum Arabic) by multi-angle laser light scattering coupled on-line to size exclusion chromatography and flow field flow fractionation. *Carbohydrate Polymers, 42*(1), 23–31. https://doi.org/10.1016/S0144-8617(99)00139-3

Piorkowski, D. T., & McClements, D. J. (2014). Beverage emulsions: Recent developments in formulation, production, and applications. *Food Hydrocolloids, 42*, 5–41. https://doi.org/10.1016/j.foodhyd.2013.07.009

Poh, B. T., & Ong, B. T. (1984). Dependence of viscosity of polystyrene solutions on molecular weight and concentration. *European Polymer Journal, 20*(10), 975–978. https://doi.org/10.1016/0014-3057(84)90080-6

Qi, W., Fong, C., & Lamport, D. T. (1991). Gum Arabic glycoprotein is a twisted hairy rope : A new model based on O-galactosylhydroxyproline as the polysaccharide attachment site. *Plant Physiology, 96*(3), 848–855. https://doi.org/10.1104/pp.96.3.848

Randall, R. C., Phillips, G. O., & Williams, P. A. (1988). The role of the proteinaceous component on the emulsifying properties of gum Arabic. *Food Hydrocolloids, 2*(2), 131–140. https://doi.org/10.1016/S0268-005X(88)80011-0

Randall, R. C., Phillips, G. O., & Williams, P. A. (1989). Fractionation and characterization of gum from *Acacia Senegal*. *Food Hydrocolloids, 3*(1), 65–75. https://doi.org/10.1016/S0268-005X(89)80034-7

Ray, A. K., Bird, P. B., Lacobucci, G. A., & Clark, B. C. (1995). Functionality of gum Arabic. Fractionation, characterization and evaluation of gum fractions in citrus oil emulsions and model beverages. *Food Hydrocolloids, 9*(2), 123–131. https://doi.org/10.1016/S0268-005X(09)80274-9

Renard, D., Garnier, C., Lapp, A., Schmitt, C., & Sanchez, C. (2012). Structure of arabinogalactan-protein from Acacia gum: From porous ellipsoids to supramolecular architectures. *Carbohydrate Polymers, 90*(1), 322–332. https://doi.org/10.1016/j.carbpol.2012.05.046

Renard, D., Lavenant-Gourgeon, L., Ralet, M.-C., & Sanchez, C. (2006). *Acacia Senegal* gum: Continuum of molecular species differing by their protein to sugar ratio, molecular weight, and charges. *Biomacromolecules, 7*(9), 2637–2649. https://doi.org/10.1021/bm060145j

Saeman, J. F., Bubl, J. L., & Harris, E. E. (1945). Quantitative saccharification of wood and cellulose. *Industrial & Engineering Chemistry Analytical Edition, 17*(1), 35–37. https://doi.org/10.1021/i560137a008

Sanchez, C., Schmitt, C., Kolodziejczyk, E., Lapp, A., Gaillard, C., & Renard, D. (2008). The acacia gum arabinogalactan fraction is a thin oblate ellipsoid: A new model based on small-angle neutron scattering and ab initio calculation. *Biophysical Journal, 94*(2), 629–639. https://doi.org/10.1529/biophysj.107.109124

Street, C. A., & Anderson, D. M. (1983). Refinement of structures previously proposed for gum Arabic and other acacia gum exudates. *Talanta, 30*(11), 887–893. https://doi.org/10.1016/0039-9140(83)80206-9

Urbat, F., Müller, P., Hildebrand, A., Wefers, D., & Bunzel, M. (2019). Comparison and optimization of different protein nitrogen quantitation and residual protein characterization methods in dietary fiber preparations. *Frontiers in Nutrition, 6*, 127. https://doi.org/10.3389/fnut.2019.00127

Van de Sande, W., & Persoons, A. (1985). The size and shape of macromolecular structures: Determination of the radius, the length and the persistance length of rod-like micelles of dodecyldimethylammonium chloride and bromide. *The Journal of Physical Chemistry, 89*(3), 404–406.

Vinayahan, T., Williams, P. A., & Phillips, G. O. (2010). Electrostatic interaction and complex formation between gum Arabic and bovine serum albumin. *Biomacromolecules, 11*(12), 3367–3374. https://doi.org/10.1021/bm100486p

Wefers, D., & Bunzel, M. (2015). Characterization of dietary fiber polysaccharides from dehulled common buckwheat (*fagopyrum esculentum*) seeds. *Cereal Chemistry, 92*(6), 598–603. https://doi.org/10.1094/CCHEM-03-15-0056-R

Williams, P. A., & Phillips, G. O. (2021). Gum Arabic. In *Handbook of hydrocolloids* (pp. 627–652). Elsevier. https://doi.org/10.1016/B978-0-12-820104-6.00022-X.

Williams, P. A., Sayers, C., Viebke, C., Senan, C., Mazoyer, J., & Boulenguer, P. (2005). Elucidation of the emulsification properties of sugar beet pectin. *Journal of Agricultural and Food Chemistry, 53*(9), 3592–3597. https://doi.org/10.1021/jf0404142

Xiang, S., Yao, X., Zhang, W., Zhang, K., Fang, Y., Nishinari, K., … Jiang, F. (2015). Gum Arabic-stabilized conjugated linoleic acid emulsions: Emulsion properties in relation to interfacial adsorption behaviors. *Food Hydrocolloids, 48*, 110–116. https://doi.org/10.1016/j.foodhyd.2015.01.033